Desalination and Water Treatment
www.deswater.com

doi: 10.1080/19443994.2015.1112840

57 (2016) 17118–17127
August

Taylor & Francis
Taylor & Francis Group

Adsorptive removal of copper (II) from aqueous solutions on phosphates: equilibrium, kinetics, and thermodynamics

L. El Fakir[a], M. Flayou[a], A. Dahchour[b], S. Sebbahi[a], F. Kifani-Sahban[c], S. El Hajjaji[a,*]

[a]*Laboratory of Spectroscopy, Molecular Modeling, Materials and Environment, Faculty of Sciences, Mohamed V University, Av Ibn Battouta, B.P. 1014, Rabat 10000, Morocco, Tel. +212 6 61 30 31 02; emails: laila_el@hotmail.fr (L. El Fakir), mflayou@onep.org.ma (M. Flayou), sebbahi_seloua@yahoo.fr (S. Sebbahi), selhajjaji@hotmail.com (S. El Hajjaji)*
[b]*Department of Fundamental and Applied Sciences, Hassan II Agronomic and Veterinary Institute, B.P. 62002, Rabat-Institute, Rabat 10000, Morocco, email: abdel_dahchour@yahoo.fr*
[c]*Laboratory of Thermodynamic and Energetic, Faculty of Sciences, Physical Department, Mohamed V University, B.P. 1014, Rabat, Morocco, email: kifani_sahban@yahoo.fr*

Received 12 March 2015; Accepted 21 October 2015

ABSTRACT

Limit of World Health Organization standard for safe amount Cu(II) in drinking water is 5 mg/L. The large usage of this material is reported to be the cause of various environmental and health hazard. Adsorption process that stands for the most common techniques due to its low cost and relative high efficiency, could perform its removal from wastewater. However, the most common adsorbents remain expensive compared with other potential natural and available adsorbents. In this work, natural and synthetic phosphates are tested for their efficacy to remove Cu(II) from contaminated water solution. Results were compared with those found with activated carbon used as reference. Effect of pH, adsorbent doses, temperature, and initial concentrations on the uptake of Cu ions by the adsorbent were examined based on statistical experimental design. Physical treatment was made to increase adsorption capacity of the tested adsorbents. The thermodynamic parameters such as free energy (ΔG°), enthalpy (ΔH°), and entropy changes (ΔS°) for the adsorption of Cu(II) were computed to predict the nature of adsorption process. Adsorption isotherms were determined and correlated with common isotherm equations such as Langmuir and Freundlich models. Adsorption data related to the two types of phosphate fit well pseudo-order model. Data confirm also net increase in adsorption with pH, adsorbent doses, while it decreases with an increase in initial concentration of copper. Variation of standard enthalpy (ΔH°) and entropy (ΔS) were beyond zero. This indicates clear tendency of the adsorption process to randomness in the solid/solution interface and reflects exothermic nature of the process, while the negative value of standard free energy variation indicates spontaneous process. Langmuir model fitted much better than the Freundlich model. These materials were found to be promising as potential adsorbents for the removal of Cu(II) from aqueous solution.

---

*Corresponding author.

Presented at the 7th International Conference on Water Resources in the Mediterranean Basin (WATMED7)
8–11 October 2014, Marrakesh, Morocco

Keywords: Activation; Adsorption; Copper; Hydroxyapatite; Experimental design; Phosphates

1. Introduction

The discharge of heavy metals into watercourses has always been a serious pollution problem, which may affect the quality of water supply [1]. Increasing concentrations of these metals in the water constitute a severe health hazard, because they are not biodegradable and can be accumulated in living tissues. Copper is a widely used metal. According to the World Health Organization, the maximum acceptable concentration of Cu(II) in drinking water is 5 mg/L [2]. Unfortunately, Cu is a persistent, bioaccumulative, and toxic chemical and is not easily metabolized. If the excessive amount of Cu(II) is allowed to enter into the environment, can cause serious health issues [3,4]. There are various methods for the removal of heavy metals, such as chemical precipitation, reverse osmosis, ion exchange, coagulation, and adsorption [2]. However, these methods are either inefficient or expensive. Adsorption is an alternative technology in which increased amount of study has been focused because of cost-effectiveness, local availability and technical feasibility for the removal of heavy metal ions from the wastewater [5]. Nevertheless, the adsorption technology in wastewater treatment is still an expensive process, mainly because of the high cost of adsorbent. Many natural and synthetic materials are used as adsorbent because of their low cost, their availability, and adsorption capacity [6,7].

In this work, we have studied adsorption efficiency of natural and synthetic phosphate for copper removal from water. Commercial activated carbon was used as reference. The effect of different parameters such as pH, adsorbent amount, temperature, and initial metal concentrations on the process has been determined by statistical experimental design. In addition, adsorption isotherms have been determined and analyzed.

2. Materials and methods

2.1. Characterization of adsorbents

Sample of natural phosphate (NP) used in this work was from Khouribga region (Morocco). The sample was washed and sieved to 100–400 mm size fraction. Hydroxyapatite (HAP) was synthesized by introducing a mass of NP into a beaker containing distilled water. The reaction of the dissolution of NP was carried out by the addition of concentrated nitric acid solution 65% (HNO_3). The mixture was maintained under shaking for 3 h at room temperature. After total dissolution of NP, the mixture obtained was filtered. The pH was adjusted to 2. Then, the obtained filtrate was neutralized with ammonium hydroxide 25% (NH_4OH). The pH of the mixture was adjusted to 10. The precipitate was left under agitation, filtered, washed with distilled water, and oven-dried at 100°C for 24 h.

NP and HAP were characterized by X-ray diffraction (XRD) using the diffractometer PHILIPS PW 13, with copper as anticathode. The spectrum of XRD shows that the untreated natural phosphate NP and synthetic apatite HAP consist on a mixture of apatite phase SiO_2-quartz and fluorite CaF_2 (Fig. 1).

The surface area of NP and HAP were determined by nitrogen (N_2) adsorption–desorption isotherms at (77 K) using an automated gas sorption system "Micrometrics ASAP 2010" instrument. The specific surface area was calculated by the Brunauer–Emmett–Teller (BET) method. The calculated surface area is about 20 and 230 m^2/g for NP and HAP respectively.

Morphological analysis of NP and HAP was performed by scanning electron microscopy (SEM). The aspect of the powders is outlined in the Fig. 2. The porosity of the surface is clearly observed.

The main chemical and structural characteristics of the two materials are presented in Table 1.

Transmission electron microscopy images of natural phosphate and hydroxyapatite were obtained with a TECNAI G2/FEI microscope. Adsorbents were

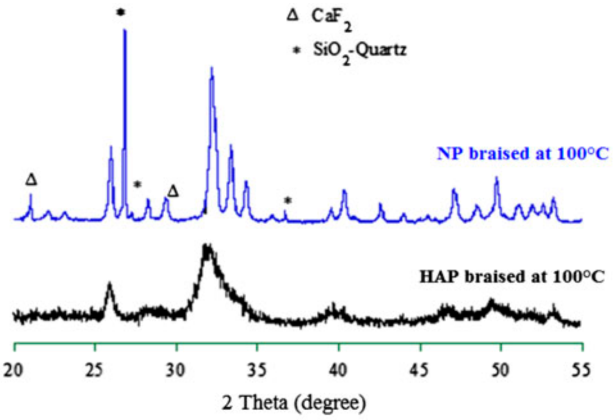

Fig. 1. XRD of natural phosphate NP and HAP.

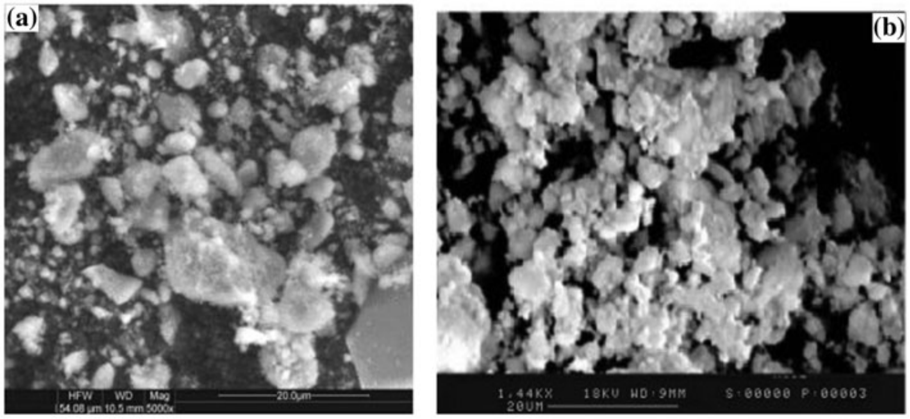

Fig. 2. SEM micrograph of (a) natural phosphate NP and (b) synthetic HAP.

Table 1
Chemical and textural characteristics of adsorbents

Sample	% Ca	Ca/P	% F	S_{BET} ($m^2\ g^{-1}$)	Crystallinity
HAP	36.60	1.60	0	230	Poor
NP	20	1.95	2.84	20	Good

deposited on a carbon-coated copper grid. TEM micrographs of NP (a), and HAP (b) were exhibited in Fig. 3. For NP sample, the smallest hexagonal phosphate particle size varies from 10 to 50 nm, which can be observed in Fig. 3(a). For HAP (Fig. 3(b)), particles are in the shape of leaves.

2.2. Experimental method

Adsorption experiments were carried out in a series of beakers filled with 100 mL of $CuSO_4{\cdot}5H_2O$ solution at different concentrations (0.1–1.2 g/L). The same amount of adsorbent (NP and HAP separately) was added separately in the flask that were shaken using a magnetic shaker for 2 h to achieve the equilibrium condition. At regular intervals, sample from the supernatant were taken out and filtered prior to determination of the remaining copper in the medium by UV–vis spectrophotometer. The maximum absorption wavelength (λ_{max}) was 800 nm. NP and HAP were further activated in air at 1,000˚C for 2 h to perform other test.

Fractional factorial designs were chosen to evaluate the factors that significantly influence adsorption of copper process. We must choose the variation limit of these factors which determines the experimental domain. For the present work, we have to evaluate

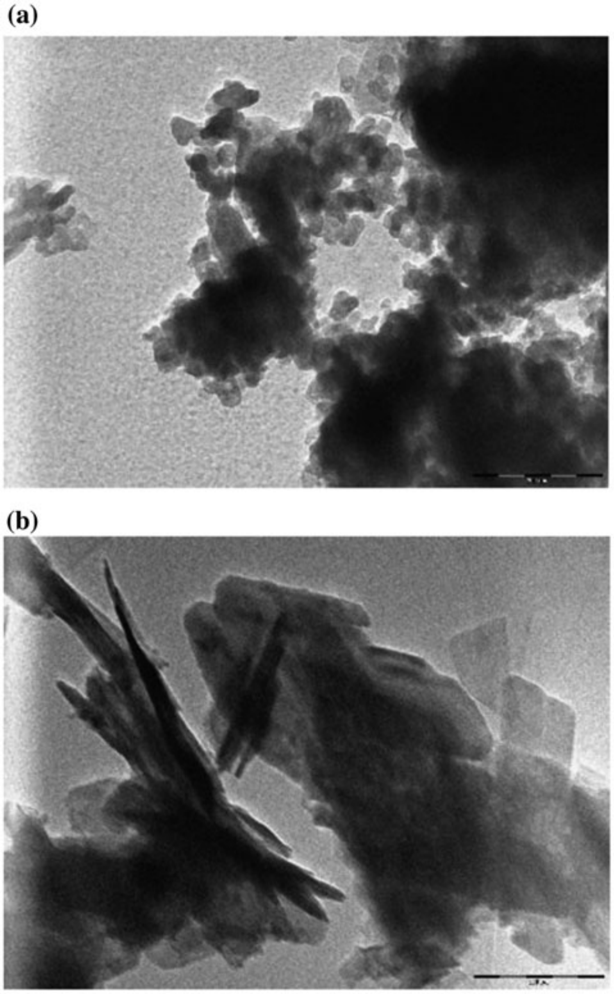

Fig. 3. TEM micrographs of (a) natural phosphate and (b) hydroxyapatite.

the influence of four factors, each at two levels (high (+1) and low (−1)). The selected parameters are pH of solution, adsorbent quantity, temperature, and initial concentration of copper. All experiments were performed in random order and the calculation was obtained by the NEMROD program [8]. In order to show the effect of each factor, the studied response is the retention rate (R%).

Retention rate was calculated as follow:

$$R\% = \frac{C_0 - C_e}{C_0} \times 100 \tag{1}$$

where C_0 and C_e are the concentrations of copper (mg L^{-1}) at $t = 0$ and $t = t_e$, respectively.

3. Results and discussion

3.1. Kinetic study

3.1.1. Before heat treatment

The contact time was evaluated as one of the most important factors affecting the adsorption efficiency. The relationship of percentage copper removal by adsorbent with contact time was plotted and presented in Fig. 4. Amount of the adsorbed metal ion increased as the time increases, and slowed down later before reaching equilibrium. There is no change in adsorption on further increase in contact time. Comparison between the three adsorbents allowed the following rank: AC > HAP > NP.

3.1.2. After heat treatment

Curves of adsorption on NP and HAP after activated at 1,000°C for 2 h are presented in Fig. 5. It appears that heat treatment significantly influences the amount of copper adsorbed. In fact, heat treatment could induce modification in physical and chemical properties of adsorbent. The uptake capacity of copper by the adsorbent and the time required for establishment of equilibrium suggest the effectiveness of these materials for wastewater treatment.

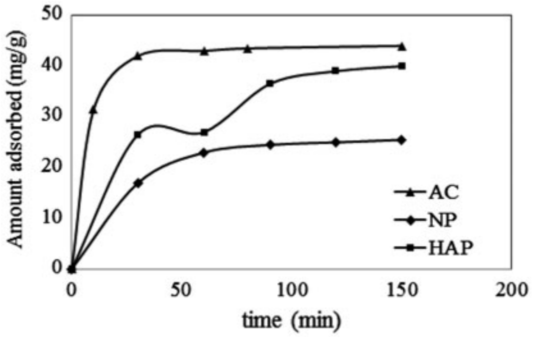

Fig. 4. Effect of contact time and nature of adsorbent on the uptake of copper ions before heat treatment.

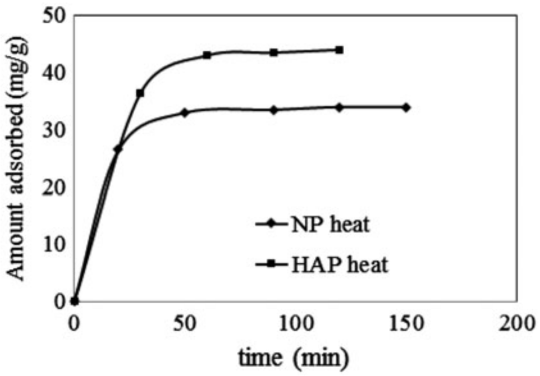

Fig. 5. Effect of contact time and nature of adsorbent on the uptake of copper ions after heat treatment.

The maximum amounts adsorbed deduced from isotherms before and after heat treatment is presented in the Table 2.

The first-order kinetic equation like Lagergren [9] and pseudo-second-order model proposed by Ho and McKay [10] equations were applied to the adsorption data.

The pseudo-first-order equation can be expressed in a linear form as:

$$\log(q_e - q_t) = \log(q_e) - K_1 \times \frac{t}{2.303} \tag{2}$$

where t (min) is the contact time, q_e and q_t are amounts of copper ions adsorbed (mg/g) at the equilibrium and at time t, respectively, and K_1 is the rate constant of adsorption (min^{-1}).

A linear form of pseudo-second-order model is shown by the following equation:

$$\frac{t}{q_t} = \frac{1}{K_2 \times q_e^2} + \frac{t}{q_e} \tag{3}$$

Table 2
The maximum amount adsorbed (q_m) for different materials studied before and after heat treatment

Adsorbents		AC	NP	HAP
q_m (ppm)	Before heat treatment	116	46	61
	After heat treatment	–	56	71

where K_2 is the rate constant of pseudo-second-order adsorption (g mg^{-1} min^{-1}).

With the plot $\log(q_e - q_t)$ vs. time, the values of K_1 can be determined. The slopes and intercepts of plots t/q_t vs. t were used to calculate the second-order rate constant K_2.

Figs. 6 and 7 show the kinetics of copper ions adsorption on NP and HAP.

The values of K_1, K_2, and R^2 clearly indicate the applicability of these kinetic equations and the pseudo-second-order nature of adsorption of copper ions on NP and HAP as shown in Table 3.

3.2. Thermodynamic study

Evaluation of thermodynamic parameters (ΔG°, ΔH°, and ΔS°) was calculated at different temperatures using the following relations [11–13]:

$$K_e = \frac{q_e}{C_e} \tag{4}$$

$$\Delta G = -RT \ln K_e \tag{5}$$

$$\ln K_e = \left(\frac{\Delta S^\circ}{R}\right) - \left(\frac{\Delta H^\circ}{R}\right)\frac{1}{T} \tag{6}$$

where K_e is the equilibrium constant, q_e is the equilibrium adsorption capacity (ppm), C_e is the concentration at equilibrium (mg/L), T is the temperature in Kelvin, and R is the gas constant.

Thermodynamic experiments were carried out at a temperature range of 298–333 K. Fig. 8 shows the plot of $\ln K_e$ vs. $1/T$ and the values of estimated thermodynamic parameters are given in Table 4.

The negative values of ΔG° confirm the feasibility of the reaction and the spontaneous nature of the sorption and the positive values of ΔH° indicate the sorption reaction to be in agreement with the endothermic nature of interaction and govern the possibility of physical adsorption [14]. Because in the case of physical adsorption, while increasing the temperature of the system, the extent of adsorption increases which rules out the possibility of chemisorption [14–17]. The enhancement of adsorption capacity of the activated carbon at higher temperatures was attributed to the enlargement of pore size and activation of the adsorbent surface [15–17]. Enhancement of the adsorption capacity of adsorbents at higher temperatures has been attributed to the enlargement of pore size and activation of adsorbents surface [15–17].

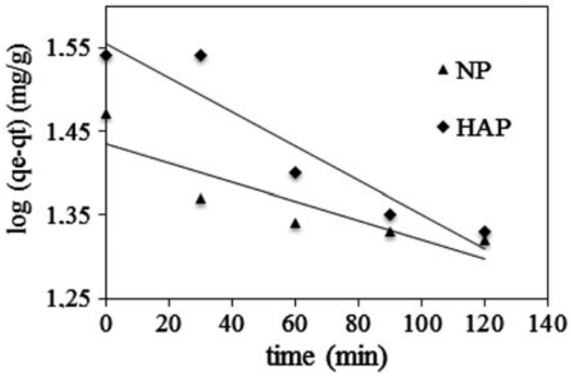

Fig. 6. Pseudo-first-order rate constants for adsorption of the copper ions onto NP and HAP.

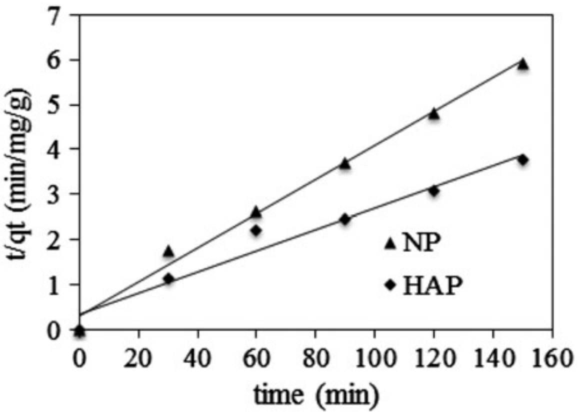

Fig. 7. Pseudo-second-order rate constants for adsorption of copper ions into NP and HAP.

3.3. Adsoption isotherms

Adsorption isotherms are essential for the description of how copper interacts with NP and HAP and are useful to optimize the use of these materials as adsorbents. Therefore, empirical equations are important to interpret and predict the adsorption data. Two types of adsorption isotherm models, namely Langmuir isotherm and Freundlich isotherm were tested.

The Langmuir isotherm is based on assuming a monolayer sorption onto a surface with a fixed number of well-defined sites. The equation is given below [18,19].

$$\frac{q_e}{q_m} = \frac{b \times C_e}{1 + b \times C_e} \tag{7}$$

where C_e is the equilibrium liquid-phase concentration (mg/L), q_e the equilibrium amount adsorbate (mg/g), q_m the maximum amount of adsorbate per unit

Table 3
Pseudo-first- and second-order rate constants for adsorption of copper ions onto NP and HAP

	Pseudo-second-order rate constants		Pseudo-first-order rate constants	
Adsorbents	R^2	K_2 (g mg^{-1} min^{-1})	R^2	K_1 (min^{-1})
NP	0.9906	0.005	0.7744	0.0025
HAP	0.9932	0.004	0.9879	0.0029

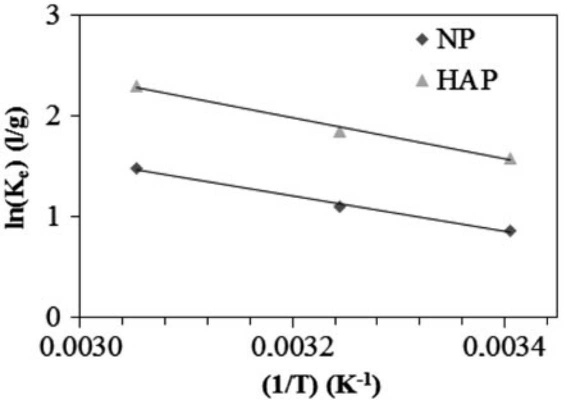

Fig. 8. The plots of ln K_e vs. $1/T$ for the adsorption of the Cu(II) ion on both NP and HAP.

Table 4
Thermodynamic parameters of copper ion sorption on NP and HAP (ΔG°, ΔH°, and ΔS°)

Adsorbents		NP	HAP
K_e	298 K	2.4039	4.9240
	313 K	3.0166	6.4269
	333 K	4.3932	9.9636
ΔH° (kJ mol^{-1})	–	14.28	16.69
ΔS° (J mol^{-1} K^{-1})	–	55.07	69.09
ΔG° (kJ mol^{-1})	298 K	−2.17	−3.95
	313 K	−2.87	−4.84
	333 K	−4.10	−6.36

sorbent (adsorbent capacity) to form a complete monolayer, and b is the Langmuir constant related to the affinity between adsorbent and adsorbate. The values can conclude that the maximum adsorption corresponds to a saturated monolayer of adsorbate molecules on adsorbent surface with constant energy and no dispersion of adsorbate in plane of the adsorbent surface [20].

The linear plots of C_e/q_e vs. C_e suggest the applicability of Langmuir isotherms shown in Fig. 9. The values of q_m and b were determined from the slopes and intercepts of the plots and are presented in Table 5.

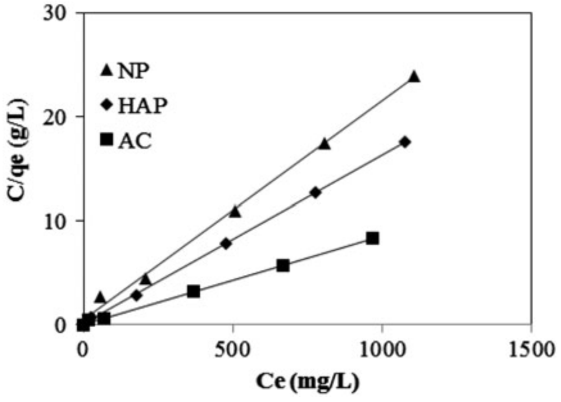

Fig. 9. Langmuir plots for copper ions adsorption onto AC, NP, and HAP.

Table 5
Parameters for Langmuir and Freundlich adsorption isotherm equation

	Langmuir			Freundlich		
	q_m	b	R	$1/n_F$	K_F	R
AC	117.6	0.102	0.999	0.218	30.1	0.637
NP	47.6	0.042	0.997	0.246	9.4	0.721
HAP	62.1	0.099	0.999	0.14	25.02	0.788

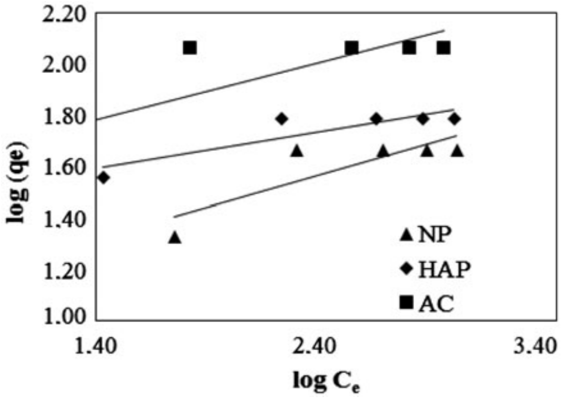

Fig. 10. Freundlich plots for copper ions adsorption onto AC, NP, and HAP.

Table 6
Fractional factorial design 2^4: theoretical values of coded variables

Exp	X_1	X_2	X_3	X_4
1	−1	−1	−1	−1
2	+1	−1	−1	−1
3	−1	+1	−1	−1
4	+1	+1	−1	−1
5	−1	−1	+1	−1
6	+1	−1	+1	−1
7	−1	+1	+1	−1
8	+1	+1	+1	−1
9	−1	−1	−1	+1
10	+1	−1	−1	+1
11	−1	+1	−1	+1
12	+1	+1	−1	+1
13	−1	−1	+1	+1
14	+1	−1	+1	+1
15	−1	+1	+1	+1
16	+1	+1	+1	+1

Freundlich model attempts to account for surface heterogeneity [21]. Freundlich isotherm model is given as follows:

$$q_e = K_F \times C_e^{1/n_F} \tag{8}$$

where K_F and n_F are Freundlich constants that are related to the adsorption capacity and intensity, respectively.

Plots of $\log q_e$ vs. $\log C_e$ are presented in Fig. 10. The values of K_F and n_F are given in Table 5.

The Langmuir model gave better fit with the experimental data than Freundlich model.

3.4. Effect of different parameters on the adsorption process

To search optimal conditions that allow optimization of adsorption phenomenon, assessment of the most influencing and passive factors was processed. This was achieved by the methodology of experimental design based on fractional factorial designs [22]. The first step consisted in the choice of the factors that can be controlled, the variation limits of these factors determines the experimental domain. In this work, we have evaluated the influence of four factors, at two levels each (high (+1) and low (−1)). A total of 16 trials were necessary (2^4) for this fractional factorial design (Table 6). All experiments were performed in random order and the calculations were performed using the NEMROD program [8].

Experimental design and the obtained results are shown in Table 7.

Processing of the data led to the estimation of 16 coefficients for the polynomial equation as follows:

$$\begin{aligned} R\ (\%) = {} & b_0 + b_1X_1 + b_2X_2 + b_3X_3 + b_4X_4 + b_{12}(X_1X_2) \\ & + b_{13}(X_1X_3) + b_{23}(X_2X_3) + b_{14}(X_1X_4) \\ & + b_{24}(X_2X_4) + b_{34}(X_3X_4) + b_{123}(X_1X_2X_3) \\ & + b_{124}(X_1X_2X_4) + b_{134}(X_1X_3X_4) + b_{234}(X_2X_3X_4) \\ & + b_{1234}(X_1X_2X_3X_4) \end{aligned}$$

Table 7
Operating conditions and retention rate R (%) on the both adsorbents

Experiences	pH	Adsorbent dosage (g)	Initial concentration (g/L)	Temperature (℃)	Retention rate (%)	
					HAP	NP
1	2 **(−1)**	0.2**(−1)**	0.1 **(−1)**	25	53	43
2	6 **(+1)**	0.2	0.1	25	86	73
3	2	1(+1)	0.1	25	63	53
4	6	1	0.1	25	91	83
5	2	0.2	1.2 **(+1)**	25	9	7
6	6	0.2	1.2	25	71	21
7	2	1	1.2	25	50	29
8	6	1	1.2	25	88	79
9	2	0.2	0.1	60	54	53
10	6	0.2	0.1	60	93	83
11	2	1	0.1	60	71	63
12	6	1	0.1	60	95	90
13	2	0.2	1.2	60	21	21
14	6	0.2	1.2	60	72	27
15	2	1	1.2	60	54	36
16	6	1	1.2	60	89	84

Note: Bold values show the experimental domain.

Table 8
Main effects and interactions effects calculated from factorial fractional design 2^4

	NP	HAP
b_0	52.9	66.3
b_1	**14.6**	**19.4**
b_2	11.8	8.9
b_3	−14.8	−9.5
b_4	4.3	2.4
b_{12}	4.7	−3.8
b_{13}	−0.1	3.9
b_{23}	7.2	4.6
b_{14}	−0.8	−0.8
b_{24}	−0.7	−0.3
b_{34}	−0.3	−0.1
b_{123}	5.2	−1.3
b_{124}	0.2	−0.1
b_{134}	−0.4	−1
b_{234}	−0.3	−0.8
b_{1234}	0.6	1.1

Note: Bold values show the most important values.

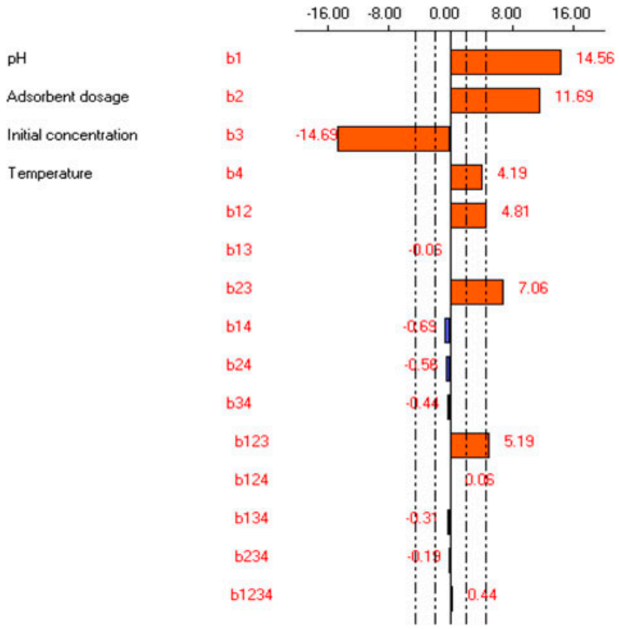

Fig. 11. Graphical analysis of the effect of different parameters on the adsorption of copper ions onto NP.

The obtained values are given in Table 8 and the graphical effect is represented in Fig. 11.

Fig. 12 represents the Pareto graphic analysis. In fact, this analysis calculates the percentage effect of each factor on the response.

Thus, in the experimental region investigated, it seems that pH is the main important parameter on the copper ions removal. Moreover, the predicted contour plots (curves of constant responses) and the three-dimensional (3D) representation of the same plots are given in Fig. 13(a) and (b), respectively. The graphic analysis of these figures confirms preceding results.

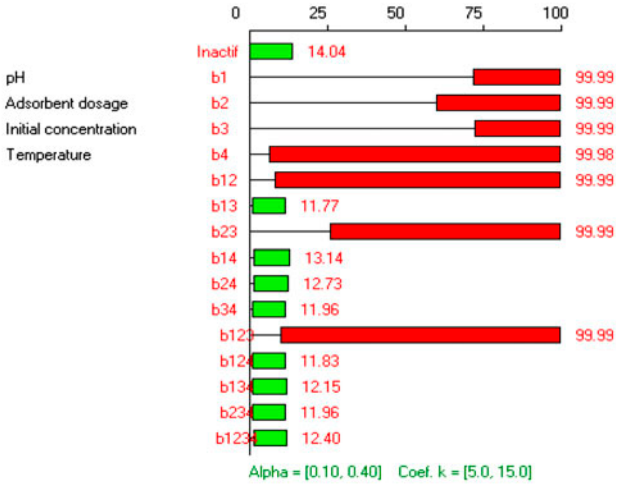

Fig. 12. Graphical Pareto analysis for NP.

The study of these results indicates that:

(1) The uptake of copper increases when the pH increases from pH 2 to 6. The minimum adsorption observed at low pH (pH 2) may be due to the higher concentration and higher mobility of H^+ ions present that favored the preferential adsorption of hydrogen ions compared with copper ions [23]. It would be plausible to suggest that at lower pH values, the surface of the adsorbent is surrounded by hydronium ions (H^+), thereby preventing the metal ions from approaching the binding sites of the sorbent [24].
(2) The adsorbent dose is another important parameter. Further increase in adsorbent dose resulted in an increase in adsorption. At higher dose of adsorbent, strong driving force and large surface area would be available for exchangeable sites for metal ions [25].
(3) The retention rate decreases by increasing the initial concentration of the copper. This is due to the availability of smaller number of surface sites on the adsorbent for a relatively larger number of adsorbing species at higher concentrations.
(4) According to the importance of the coefficients, the effect of pH on the retention rate of copper ions appears as being the most important.

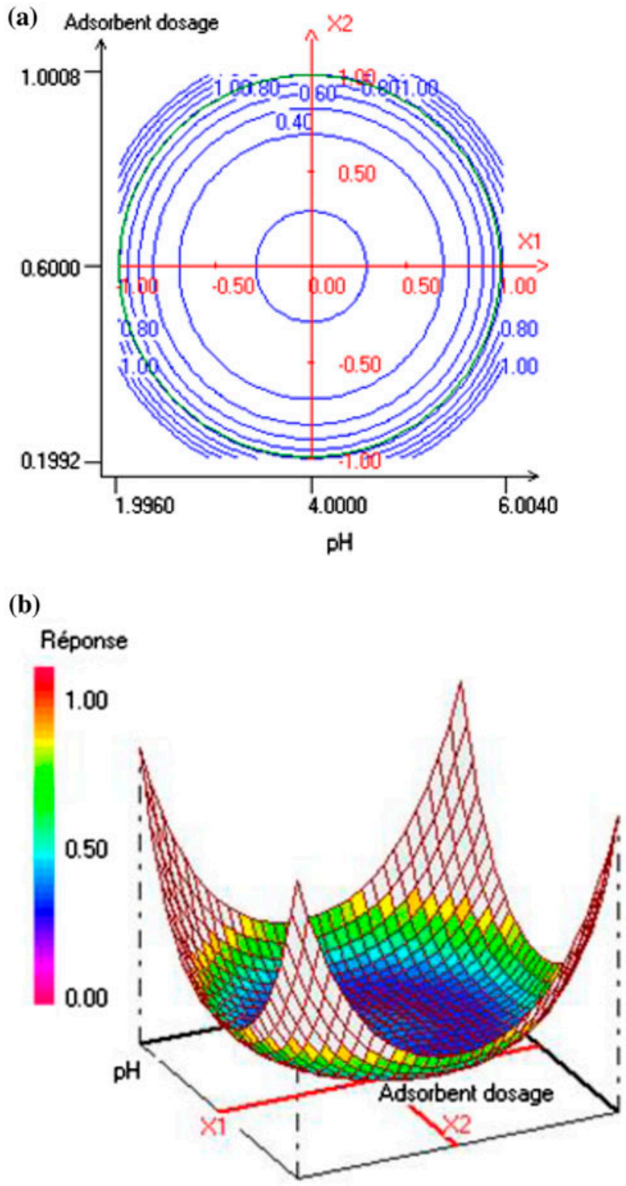

Fig. 13. (a) Contour plots of copper ions removal vs. the adsorbent dosage (g) and pH; (b) corresponding three-dimensional plot; results obtained from Doehlert design. Initial concentration = 0.65 g/L and temperature = 42.5˚C.

4. Conclusion

This study has investigated the adsorption of copper by different adsorbents, namely NP and HAP; commercial AC was used as a reference. Heat treatment induces an improvement in retention of the studied ion metal. Adsorption of copper ions onto NP and HAP follows the second-order rate kinetics. The Langmuir isotherm model was the most appropriate to describe the adsorption of the copper ions on the NP and HAP than Freundlich model. Studies of the effect of different parameters on the adsorption of copper ions using the experimental design methodology showed that retention rate *R* increased with pH, adsorbent dose, and temperature and decreased when initial concentration of copper ions increased. These results are in favor of using studied materials as potential adsorbents the removal of copper and other metal ions from wastewater.

Acknowledgement

We thank the “National Center for Scientific and Technical Research” in Rabat (Morocco) for their support by the Excellence Scholarship.

References

[1] N.D. Tumin, A.L. Chuah, Z. Zawani, S.A. Rashid, Adsorption of copper from aqueous solution by Elais Guineensis kernel activated carbon, J. Eng. Sci. Technol. 3 (2008) 180–189.

[2] A. Ahmadpour, M. Tahmasbi, T. Bastami, J.A. Besharati, Rapid removal of cobalt ion from aqueous solutions by almond green hull. J. Hazard. Mater. 166 (2009) 925–930.

[3] B. Zhu, T. Fan, D. Zhang, Adsorption of copper ions from aqueous solution by citric acid modified soybean straw, J. Hazard. Mater. 153 (2008) 300–308.

[4] M.O. Amdur, J. Doull, C.D. Klaassen (Eds.), Casarett and Doull’s Toxicology—The Basic Science of Poisons. fourth ed., Pergamon Press, Elmsford, New York, 1991.

[5] R. Bazargan-Lari, M.E. Bahrololoom, A. Nemati, Dependence of equilibrium, kinetics and thermodynamics of Zn(II) ions sorption from water on particle size of natural hydroxyapatite extracted from bone ash, Int. Scholarly Sci. Res. Innovation 6 (2012) 959–964.

[6] M. Sarioglu, Ü.A. Atay, Y. Cebeci, Removal of copper from aqueous solutions by phosphate rock, Desalination 181 (2005) 303–311.

[7] L. El Fakir, M. Flayou, H. Cherkoui, N. Saoudi, A. Dahchour, S. Sebbahi, M.A. El Mhammedi, S. El Hajjaji, Study of adsorptive removal of copper(II) capacity from aqueous solutions on phosphates, Mater. Environ. Sci. 5(S1) (2014) 2107–2112.

[8] D. Mathieu, R. Phan-Tan-Luu, NEMROD®, SoftwareLPRAI, Marseille, France, 1995.

[9] S. Lagergren, About the theory of so called adsorption of soluble substances. K. Sven. Vetenskapsakad. Handlingnaar, Band. 24 (1898) 1–39.

[10] Y.S. Ho, G. McKay, Pseudo-second order model for sorption processes, Process Biochem. 34 (1999) 451–465.

[11] X. Cao, L.Q. Ma, D.R. Rhue, C.S. Appel, Mechanisms of lead, copper and zinc retention by phosphate rocks, Environ. Pollut. 131 (2004) 435–444.

[12] J. Jeanjean, U. Vincent, M. Fedoroff, Structural modification of calcium hydroxyapatite induced by sorption of cadmium ions, J. Solid State Chem. 108 (1994) 68–72.

[13] M.E. Bahrololoom, M. Javidi, S. Javadpour, J. Ma, Characterisation of natural hydroxyapatite extracted from bovine cortical bone ash. J. Ceram. Process. Res. 10 (2009) 129–138.

[14] I. Mobasherpour, E. Salahi, M. Ebrahimi, Thermodynamics and kinetics of adsorption of Cu(II) from aqueous solutions onto multi-walled carbon nanotubes, J. Saudi Chem. Soc. 18 (2014) 792–801.

[15] S. Arivoli, M. Hema, Comparative study on the adsorption kinetics and thermodynamics of dyes onto acid activated low cost carbon, Int. J. Phys. Sci. 2 (2007) 10–17.

[16] S. Arivoli, B.R. Venkatraman, T. Rajachandrasekar, M. Hema, Adsorption of ferrous ion from aqueous solution by low cost activated carbon obtained from natural plant material, Res. J. Chem. Environ. 17 (2007) 70–78.

[17] S. Arivoli, K. Kalpana, R. Sudha, T. Rajachandrasekar, Comparative study on the adsorption kinetics and thermodynamics of metal ions onto acid activated low cost carbon, E J. Chem 4 (2007) 238–254.

[18] M.I. Kandah, Zinc and cadmium adsorption on low-grade phosphate, Sep. Purif. Technol. 35(1) (2004) 61–70.

[19] L. Norton, K. Baskaran, T. McKenzie, Biosorption of zinc from aqueous solutions using biosolids, Adv. Environ. Res. 8(3–4) (2004) 629–635.

[20] R. Prabakaran, S. Arivoli, M. Hema, C. Kamatchi, Removal of copper ion from aqueous solutions by low cost activated carbon from *Thespesia populnea* Bark, J. Chem. Pharm. Res. 3(5) (2011) 532–543.

[21] T. Shahwan, H.N. Erten, Thermodynamic parameters of Cs^+ sorption on natural clays, J. Radioanal. Nucl. Chem. 253(1) (2002) 115–120.

[22] G.E.P. Box, W.G. Hunter, J.S. Hunter, Statistics for Experimenters: An Introduction to Design Data Analysis and Model Building, Wiley, New York, NY, 1978.

[23] M. Ajmal, R.A.K. Rao, R. Ahmad, J. Ahmad, Adsorption studies on *Citrus reticulata* (fruit peel of orange): removal and recovery of Ni(II) from electroplating wastewater, J. Hazard. Mater. 79(1–2) (2000) 117–131.

[24] K.K. Wong, C.K. Lee, K.S. Low, M.J. Haron, Removal of Cu and Pb by tartaric acid modified rice husk from aqueous solutions, Chemosphere 50 (2003) 23–28.

[25] S. Babel, T.A. Kurniawan, Cr(VI) removal from synthetic wastewater using coconut shell charcoal and commercial activated carbon modified with oxidizing agents and/or chitosan, Chemosphere 54 (2004) 951–967.